JACS
JOURNAL OF THE AMERICAN CHEMICAL SOCIETY
Communication
pubs.acs.org/JACS

Compositional Dependence of the Open-Circuit Voltage in Ternary Blend Bulk Heterojunction Solar Cells Based on Two Donor Polymers

Petr P. Khlyabich, Beate Burkhart, and Barry C. Thompson*

Department of Chemistry and Loker Hydrocarbon Research Institute, University of Southern California, Los Angeles, California 90089-1661, United States

Supporting Information

ABSTRACT: Ternary blend bulk heterojunction (BHJ) solar cells containing as donor polymers two P3HT analogues, high-band-gap poly(3-hexylthiophene-*co*-3-(2-ethylhexyl)thiophene) ($P3HT_{75}$-*co*-EHT_{25}) and low-band-gap poly(3-hexylthiophene−thiophene−diketopyrrolopyrrole) (P3HTT-DPP-10%), with phenyl-C_{61}-butyric acid methyl ester ($PC_{61}BM$) as an acceptor were studied. When the ratio of the three components was varied, the open-circuit voltage (V_{oc}) increased as the amount of $P3HT_{75}$-*co*-EHT_{25} increased. The dependence of V_{oc} on the polymer composition for the ternary blend regime was linear when the overall polymer:fullerene ratio was optimized for each polymer:polymer ratio. Also, the short-circuit current densities (J_{sc}) for the ternary blends were bettter than those of the binary blends because of complementary polymer absorption, as verified using external quantum efficiency measurements. High fill factors (FF) (>0.59) were achieved in all cases and are attributed to high charge-carrier mobilities in the ternary blends. As a result of the intermediate V_{oc}, increased J_{sc} and high FF, the ternary blend BHJ solar cells showed power conversion efficiencies of up to 5.51%, exceeding those of the corresponding binary blends (3.16 and 5.07%). Importantly, this work shows that upon optimization of the overall polymer:fullerene ratio at each polymer:-polymer ratio, high FF, regular variations in V_{oc}, and enhanced J_{sc} are possible throughout the ternary blend composition regime. This adds to the growing evidence that the use of ternary blends is a general and effective strategy for producing efficient organic photovoltaics manufactured in a single active-layer processing step.

Extensive research on bulk heterojunction (BHJ) solar cells in the past decade has resulted in deep understanding of the operating principles of binary blend solar cells composed of a polymeric donor and a fullerene acceptor.[1] Numerous polymers have been synthesized,[2,3] and efficiencies exceeding 8% have been achieved.[4] As an approach for further increasing the power conversion efficiency, tandem solar cells, in which two (or more) subcells absorbing light in different regions of the solar spectrum are connected either in series or parallel, were studied.[5] Despite the increase in either the open-circuit voltage (V_{oc})[5c] or the short-circuit current density (J_{sc}),[5b] only slightly higher efficiencies were obtained with tandem cells.[6] In addition, tandem cells require more complex design and fabrication and cannot be manufactured in a single active-layer processing step,[5b,c] in contrast to the desire for inexpensive solar cells.[1d] Importantly, the efficiencies (η) achieved with the described strategies are approaching their theoretical limits of 10−12% for binary solar cells[1a,7] and 14−15% for tandem solar cells with two absorbing layers.[5b,c,7b]

We recently demonstrated for the first time that the V_{oc} of ternary blend BHJ solar cells based on one donor and two acceptors is composition-dependent and can be tuned across the full range defined by the corresponding limiting binary blends without negatively impacting the fill factor (FF) or the J_{sc}.[8] This finding opened the door to BHJ solar cells with the potential to exceed the efficiency limit, even for tandem cells, but fabricated in a single active layer processing step. Following our initial discovery of the potential of ternary blend BHJ solar cells and our prediction of increased efficiency with a judicious choice of donor polymers and a fullerene acceptor,[8] You and co-workers recently demonstrated that blends of two donor polymers and a fullerene acceptor, at constant overall polymer:fullerene ratio, could exceed the efficiency of the limiting binary blends via an increase in J_{sc} and modulation of V_{oc}.[9] However, a vast number of fundamental questions remain to be answered, as there is no clear set of structure−function relationships for component selection and the mechanism of operation has not been established.

Here we investigated the composition dependence of V_{oc} in a ternary blend system based on two donor polymers and a fullerene acceptor for which the limiting binary blends do not give optimal performance at the same polymer:fullerene ratio. We also sought to demonstrate the generality of this ternary blend approach. The model ternary blend system used here (Figure 1) consisted of two donor polymers, high-band-gap poly(3-hexylthiophene-*co*-3-(2-ethylhexyl)thiophene) ($P3HT_{75}$-*co*-EHT_{25})[10a] and low-band-gap poly(3-hexylthiophene−thiophene−diketopyrrolopyrrole) (P3HTT-DPP-10%),[10b] and phenyl-C_{61}-butyric acid methyl ester ($PC_{61}BM$) as the acceptor. The overall polymer:fullerene ratio of the ternary blend BHJ solar cells was individually optimized at each polymer:polymer ratio. In this case, we observed that even the smallest amount of the second polymer in the ternary blend had a large effect on V_{oc}, which evolved linearly with composition across the ternary blend regime. When the overall polymer:fullerene ratio was not individually optimized at each polymer:polymer ratio, a significant decrease in V_{oc} and a

Received: March 26, 2012
Published: May 15, 2012

   dx.doi.org/10.1021/ja302935n | *J. Am. Chem. Soc.* 2012, 134, 9074−9077

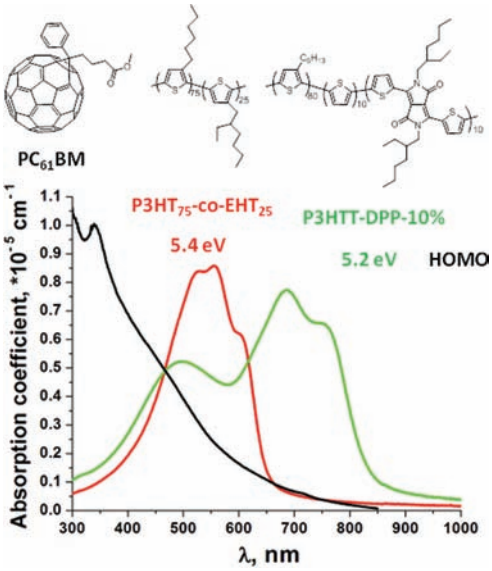

Figure 1. Structures, HOMO energies, and absorption profiles of $PC_{61}BM$, $P3HT_{75}$-*co*-EHT_{25}, and P3HTT-DPP-10%.

deviation from linearity in the ternary blend regime were observed, accompanied by decreases in J_{sc}, FF, and η.

The choice of donor polymers was dictated by the desire to simultaneously increase J_{sc} through complementary absorption and to have an intermediate V_{oc} in the ternary blends. As shown in Figure 1, P3HTT-DPP-10%, $P3HT_{75}$-*co*-EHT_{25}, and $PC_{61}BM$ provide broad and uniformly strong absorption from 300 to 830 nm, which should facilitate an increase in J_{sc} with respect to either binary blend solar cell. At the same time, the difference in the HOMO energies of $P3HT_{75}$-*co*-EHT_{25} (5.4 eV[10a]) and P3HTT-DPP-10% (5.2 eV[10b]) should enable V_{oc} tunability in the ternary blend solar cells at different polymer ratios. Furthermore, high efficiencies were obtained in both binary blend solar cells.[10] Importantly, both semi random[10b,11] P3HTT-DPP-10% and random P3HT-*co*-EHT[10a] are P3HT analogues containing 80 and 75% 3HT repeat units, respectively. Copolymerization allowed us to tune the band gap of P3HTT-DPP-10% and the HOMO energy of $P3HT_{75}$-*co*-EHT_{25} relative to P3HT in order to give a complementary set of properties ideal for analyzing the behavior of the ternary blends in the context of a "P3HT:PCBM" model system, enabling the use of similar processing conditions at each composition.

Photovoltaic devices containing ternary blends in a conventional device configuration, ITO/PEDOT:PSS/P3HTT-DPP-10%:$P3HT_{75}$-*co*-EHT_{25}:$PC_{61}BM$/Al, were fabricated in air. The ternary blend BHJ solar cells were optimized at each polymer:polymer ratio to obtain the highest efficiencies. Optimal processing conditions included slow solvent evaporation (solvent annealing) from the P3HTT-DPP-10%:$P3HT_{75}$-*co*-EHT_{25}:$PC_{61}BM$ blends after spin-coating and prior to Al deposition. The optimization of solar cells at each ternary composition was based on the same empirical principles that govern the optimization of well-known binary blend solar cells,[12] differing only in the number of variables that must be optimized and thus requiring the fabrication of a correspondingly larger number of solar cells in the process. Table 1 lists the optimized average values of J_{sc}, V_{oc}, FF, and η obtained under simulated AM 1.5G illumination (100 mW/cm^2) as the P3HTT-DPP-10%:$P3HT_{75}$-*co*-EHT_{25} ratio was varied. As

Table 1. Photovoltaic Properties of the Ternary Blend BHJ Solar Cells at the Optimized Ratios

P3HTT-DPP-10%: $P3HT_{75}$-*co*-EHT_{25}:$PC_{61}BM$[a]	J_{sc} (mA/cm^2)	V_{oc} (V)	FF	η (%)
1:0:1.3	14.38	0.574	0.62	5.07
0.9:0.1:1.1[b]	15.05	0.603	0.61	5.51
0.8:0.2:1.0[b]	14.60	0.608	0.61	5.37
0.7:0.3:1.0[c]	11.54	0.614	0.59	4.15
0.6:0.4:1.0[c]	11.19	0.619	0.59	4.12
0.5:0.5:0.9	10.89	0.622	0.59	4.00
0.4:0.6:0.9	10.19	0.626	0.59	3.74
0.3:0.7:0.8	9.77	0.633	0.59	3.64
0.2:0.8:0.8	8.57	0.639	0.60	3.27
0.1:0.9:0.9	8.25	0.646	0.59	3.10
0:1:0.8[d]	7.96	0.675	0.59	3.16

[a]All devices were spin-coated from *o*-dichlorobenzene and placed into the N_2 cabinet before aluminum deposition for 30 min, unless otherwise noted. [b]60 min. [c]45 min. [d]20 min.

shown in Table 1, the overall polymer:fullerene ratio of the individually optimized ternary blend solar cells tracked regularly with the P3HTT-DPP-10%:$P3HT_{75}$-*co*-EHT_{25} ratio. Efficiencies of the ternary blends increased noticeably by 0.44% and 0.30%, going from 5.07% with P3HTT-DPP-10%:$PC_{61}BM$ to 5.51 and 5.37% at P3HTT-DPP-10%:$P3HT_{75}$-*co*-EHT_{25}:$PC_{61}BM$ ratios of 0.9:0.1:1.1 and 0.8:0.2:1.0, respectively. Furthermore, at all other three-component ratios except 0.1:0.9:0.9 (where the J_{sc} increase was smaller than the V_{oc} decrease relative to 0:1:0.8), the power conversion efficiencies were higher than for the binary $P3HT_{75}$-*co*-EHT_{25}:$PC_{61}BM$ solar cell. This observation supports the use of ternary blend BHJ solar cells as an effective way to overcome the efficiency limits of the corresponding binary blend solar cells.

Another interesting observation from Table 1, also illustrated in Figure 2a, is that V_{oc} in the individually optimized ternary blends is composition-dependent, as was shown for the case of one donor and two acceptors in earlier papers.[8,13] A noticeable difference from the previous results is the specific evolution of V_{oc}. Upon introduction of the second polymer component into either limiting polymer:fullerene binary blend, V_{oc} rapidly changed by 29 mV. After this, in the ternary blend composition regime, V_{oc} increased linearly from 0.603 to 0.646 V as the fraction of $P3HT_{75}$-*co*-EHT_{25} (with the lower-lying HOMO) increased. On the other hand, as shown in Figure 2b, when the overall polymer:fullerene ratio was not individually optimized at each polymer:polymer ratio but rather held constant, a significant decrease in V_{oc} and a deviation from linearity in the ternary blend composition regime were observed. When the overall polymer:$PC_{61}BM$ ratio in the ternary blend was fixed at 1:1.1, a linear dependence of V_{oc} on the composition was observed, except for the case of 10% $P3HT_{75}$-*co*-EHT_{25}, which was the optimal overall polymer:fullerene ratio. Across the remaining composition range, the V_{oc} values were significantly lower than for the individually optimized ternary blends. A nonlinear dependence of V_{oc} on the ternary blend composition was observed for a fixed overall polymer:$PC_{61}BM$ ratio of 1:1.0. Here, linear behavior at $P3HT_{75}$-*co*-EHT_{25} loadings below 50% was followed by a saturation regime with almost constant V_{oc} up to a loading of 80% and then an increase at higher loadings. Importantly, all cases where the overall polymer:fullerene ratio was not individually optimized at each polymer:polymer ratio were accompanied by decreases in J_{sc}, FF, and η [see the

dx.doi.org/10.1021/ja302935n | J. Am. Chem. Soc. 2012, 134, 9074−9077

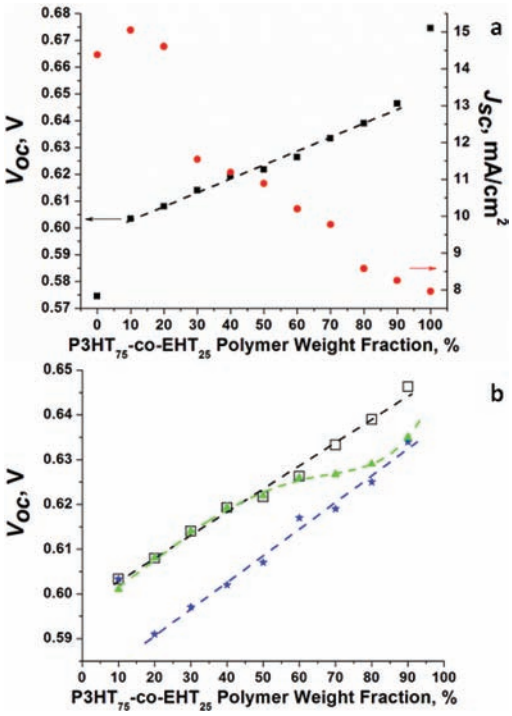

Figure 2. (a) V_{oc} (black ■, left axis) and J_{sc} (red ●, right axis) for individually optimized ternary blend BHJ solar cells containing different fractions of P3HT$_{75}$-*co*-EHT$_{25}$ (Table 1). (b) V_{oc} for individually optimized ternary blend solar cells (□) and cells with fixed overall polymer:PC$_{61}$BM ratios of 1:1.1 (blue ★) and 1:1.0 (green ▲).

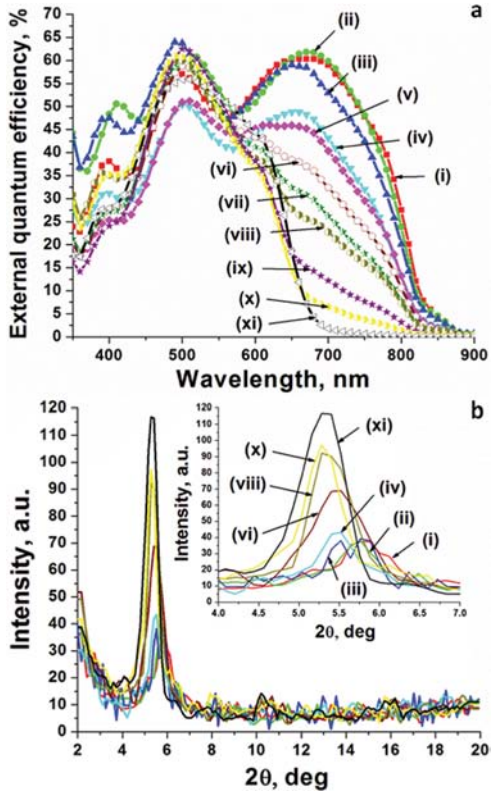

Figure 3. (a) EQEs of ternary blend BHJ solar cells and (b) GIXRD patterns of thin films with various ternary blend ratios: (i) 1:0:1.3 (red), (ii) 0.9:0.1:1.1 (green), (iii) 0.8:0.2:1.0 (blue), (iv) 0.7:0.3:1.0 (cyan), (v) 0.6:0.4:1.0 (magenta), (vi) 0.5:0.5:0.9 (wine-red), (vii) 0.4:0.6:0.9 (olive), (viii) 0.3:0.7:0.8 (dark-yellow), (ix) 0.2:0.8:0.8 (purple), (x) 0.1:0.9:0.9 (yellow), and (xi) 0:1:0.8 (black).

Supporting Information (SI)]. This implies that individual optimization of the overall composition at each polymer:-polymer ratio is necessary to achieve maximum efficiency in ternary blend solar cells and that a significant increase in V_{oc} can be achieved upon the introduction of even small amounts of a donor polymer with a lower-lying HOMO.

In contrast to the V_{oc} trend observed in Table 1, J_{sc} was found first to increase and then to decrease with increasing P3HT$_{75}$-*co*-EHT$_{25}$ content (Figure 2a) but still remained higher than that in P3HT$_{75}$-*co*-EHT$_{25}$:PC$_{61}$BM solar cells in all cases. This is explained by the complementary absorption of the P3HTT-DPP-10%:P3HT$_{75}$-*co*-EHT$_{25}$:PC$_{61}$BM blend (Figure 1). Inclusion of 10−20% high-band-gap P3HT$_{75}$-*co*-EHT$_{25}$ in the ternary blend increased the absorption coefficient in the 400−600 nm region (see the SI), while the intensity of the long-wavelength absorption due to P3HTT-DPP-10% remained almost the same. Moreover, the position of the peak in the high-energy region was red-shifted as the fraction of P3HT$_{75}$-*co*-EHT$_{25}$ increased, while that of the long-wavelength peak remained the same. As a result, the number of absorbed photons and thus J_{sc} increased. Upon addition of >30% P3HT$_{75}$-*co*-EHT$_{25}$, the absorption in the long-wavelength region decreased dramatically, while that in the visible region increased significantly. Therefore, fewer low-energy photons were absorbed, causing a decrease in J_{sc}.

To investigate further the origin of the J_{sc} changes in the ternary blend solar cells, external quantum efficiencies (EQEs) were measured (Figure 3a). P3HTT-DPP-10%:PC$_{61}$BM and P3HT$_{75}$-*co*-EHT$_{25}$:PC$_{61}$BM binary blend solar cells have strong photoresponse in the 400−800 nm and 400−650 nm regions, respectively. Addition of 10−20% P3HT$_{75}$-*co*-EHT$_{25}$ to P3HTT-DPP-10%:PC$_{61}$BM increased the EQE in the visible region of the solar spectrum while keeping the long-wavelength photoresponse from P3HTT-DPP-10% unchanged. Therefore, an enhanced J_{sc} was recorded for ratios of 0.9:0.1:1.1 and 0.8:0.2:1.0. The thickness of each device was optimized to obtain the best overall efficiency and FF. This required film thicknesses of 75 nm for the binary blend solar cells and 85−90 nm for the ternary blend solar cells. Consistent with the absorption profiles, further increases in the P3HT$_{75}$-*co*-EHT$_{25}$ content in the ternary blend decreased the photocurrent generated by P3HTT-DPP-10%, thus decreasing J_{sc}.

To gain deeper insight, the morphology was also investigated. P3HTT-DPP-10% and P3HT$_{75}$-*co*-EHT$_{25}$ were semicrystalline with (100) interchain distances of 15.07 and 16.72 Å, respectively (see the SI). In the binary blends, the polymers retained their semicrystalline nature, as can be seen from the presence of the vibronic shoulders in the UV−vis spectra[14] (see the SI) and from the grazing-incidence X-ray diffraction (GIXRD) data shown in Figure 3b. In the ternary blends, both polymers remained semicrystalline, and two peaks were present for the 0.8:0.2:1.0 ratio in the GIXRD profile [Figure 3b(iii)]. Furthermore, vibronic shoulders for both polymers were present in the UV−vis spectra of the P3HTT-DPP-10%:P3HT$_{75}$-*co*-EHT$_{25}$:PC$_{61}$BM ternary blends (see the SI). The interchain distances for the P3HTT-DPP-10% and P3HT$_{75}$-*co*-EHT$_{25}$ domains changed in opposite directions as the fraction of P3HT$_{75}$-*co*-EHT$_{25}$ in the ternary blend increased. The interchain distance for P3HTT-DPP-10% increased from 15.27 Å for 1:0:1.3 to 15.41 Å for 0.8:0.2:1.0,

dx.doi.org/10.1021/ja302935n | J. Am. Chem. Soc. 2012, 134, 9074−9077

while P3HT$_{75}$-*co*-EHT$_{25}$ was packed tighter, with the interchain distance decreasing from 16.69 Å for 0:1:0.8 to 16.02 Å for 0.8:0.2:1.0. The ability of both polymers to remain semicrystalline and pack closer in the ternary blends should contribute to the high J_{sc} observed in the ternary blend solar cells.

Finally, high FF values (>0.59) were observed at all optimized ternary blend ratios (Table 1). This can be attributed to balanced, trap-free charge transport through the bulk[15] and favorable morphology.[16] Hole mobilities for the binary and ternary blends were in the range from 1.11×10^{-3} to 3.23×10^{-3} cm^2 V^{-1} s^{-1}, increasing with greater fraction of P3HTT-DPP-10% (see the SI). These values are close to the literature values for solvent-annealed P3HT:PC$_{61}$BM binary blends.[17] High values can be also attributed to the ability of both polymers to retain their semicrystalline nature in the ternary blends. Transmission electron microscopy (TEM) images (see the SI) showed similar bicontinious blends with nanometer-scale phase separation at different P3HTT-DPP-10%:P3HT$_{75}$-*co*-EHT$_{25}$:PC$_{61}$BM ratios. As a result, the introduction of the third component in the blend does not change the overall polymer:fullerene morphology, suggesting no negative impact on charge transport through the ternary blends. However, this result raises important questions about the detailed lateral and vertical phase separation of the three components and emphasizes the importance of detailed investigations of the morphology in ternary blend systems.[18]

In summary, we have fabricated ternary blend BHJ solar cells containing two donor polymers, P3HT$_{75}$-*co*-EHT$_{25}$ and P3HTT-DPP-10%, and PC$_{61}$BM as the acceptor. The overall polymer:fullerene ratio of the ternary blend BHJ solar cells was individually optimized at each polymer:polymer ratio. This individual optimization was necessary to obtain a simultaneous increase in J_{sc}, intermediate V_{oc}, high FF, and high η. Furthermore, we observed that the introduction of even the smallest amount of the second polymer into either limiting polymer:fullerene binary blend had a large effect on V_{oc}, and for the present system, V_{oc} evolved linearly with composition across the ternary blend regime for the optimized case. When the overall polymer:fullerene ratio was not individually optimized at each polymer:polymer ratio, a significant decrease in V_{oc} and a deviation from linearity in the ternary blend composition regime were observed, accompanied by decreases in J_{sc}, FF, and η. Overall, the results of this work support the growing evidence that the use of ternary blend BHJ solar cells is an effective strategy for producing more efficient organic photovoltaics manufactured in a single active-layer processing step, with the possibility of exceeding the power conversion efficiency limits for binary blend solar cells. The results presented here also demonstrate that a judicious choice of paired components with smaller band gaps and lower-lying HOMO energies must be accompanied by careful optimization of the film composition and processing if the potentially paradigm-shifting nature of this platform is to be realized. Moving forward, it will be necessary to pursue detailed physical models of ternary blend systems to gain insight into the relationship between the morphology and the electronic structure of the components in order to exploit fully the potential of the ternary blend approach.

■ ASSOCIATED CONTENT

Supporting Information

Solar cell fabrication and additional data. This material is available free of charge via the Internet at http://pubs.acs.org.

■ AUTHOR INFORMATION

Corresponding Author

barrycth@usc.edu

Notes

The authors declare no competing financial interest.

■ ACKNOWLEDGMENTS

This material is based on work supported as part of the Center for Energy Nanoscience, an Energy Frontier Research Center funded by DOE BES (DE-SC0001013), specifically for support of P.P.K. Acknowledgement is made to the donors of the ACS PRF for support of B.B. (49734-DNI10).

■ REFERENCES

(1) (a) Thompson, B. C.; Khlyabich, P. P.; Burkhart, B.; Aviles, A. E.; Rudenko, A.; Shultz, G. V.; Ng, C. F.; Mangubat, L. B. *Green* **2011**, *1*, 29. (b) Schlenker, C. W.; Thompson, M. E. *Chem. Commun.* **2011**, *47*, 3702. (c) Clarke, T. M.; Durrant, J. R. *Chem. Rev.* **2010**, *110*, 6736. (d) Deibel, C.; Dyakonov, V. *Rep. Prog. Phys.* **2010**, *73*, 096401. (e) Brédas, J.-L.; Norton, J. E.; Cornil, J.; Coropceanu, V. *Acc. Chem. Res.* **2009**, *42*, 1691. (f) Beaujuge, P. M.; Fréchet, J. M. J. *J. Am. Chem. Soc.* **2011**, *133*, 20009.

(2) Chochos, C. L.; Choulis, S. A. *Prog. Polym. Sci.* **2011**, *36*, 1326.

(3) Boudreault, P.-L. T.; Najari, A.; Leclerc, M. *Chem. Mater.* **2011**, *23*, 456.

(4) (a) Small, C. E.; Chen, S.; Subbiah, J.; Amb, C. M.; Tsang, S.-W.; Lai, T.-H.; Reynolds, J. R.; So, F. *Nat. Photonics* **2011**, *6*, 115. (b) He, Z.; Zhong, C.; Huang, X.; Wong, W.-Y.; Wu, H.; Chen, L.; Su, S.; Cao, Y. *Adv. Mater.* **2011**, *23*, 4636. (c) Green, M. A.; Emery, K.; Hishikawa, Y.; Warta, W.; Dunlop, E. D. *Prog. Photovoltaics* **2011**, *19*, 565.

(5) (a) Sista, S.; Hong, Z.; Chen, L.-M.; Yang, Y. *Energy Environ. Sci.* **2011**, *4*, 1606. (b) Siddiki, M. K.; Li, J.; Galipeau, D.; Qiao, Q. *Energy Environ. Sci.* **2010**, *3*, 867. (c) Ameri, T.; Dennler, G.; Lungenschmied, C.; Brabec, C. J. *Energy Environ. Sci.* **2009**, *2*, 347.

(6) Dou, L.; You, J.; Yang, J.; Chen, C.-C.; He, Y.; Murase, S.; Moriarty, T.; Emery, K.; Li, G.; Yang, Y. *Nat. Photonics* **2012**, *6*, 180.

(7) (a) Nayak, P. K.; Garcia-Belmonte, G.; Kahn, A.; Bisquert, J.; Cahen, D. *Energy Environ. Sci.* **2012**, *5*, 6022. (b) Kotlarski, J. D.; Blom, P. W. M. *Appl. Phys. Lett.* **2011**, *98*, 053301. (c) Veldman, D.; Meskers, S. C. J.; Janssen, R. A. J. *Adv. Funct. Mater.* **2009**, *19*, 1939. (d) Kippelen, B.; Brédas, J.-L. *Energy Environ. Sci.* **2009**, *2*, 251.

(8) Khlyabich, P. P.; Burkhart, B.; Thompson, B. C. *J. Am. Chem. Soc.* **2011**, *133*, 14534.

(9) Yang, L.; Zhou, H.; Price, S. C.; You, W. *J. Am. Chem. Soc.* **2012**, *134*, 5432.

(10) (a) Burkhart, B.; Khlyabich, P. P.; Thompson, B. C. *Macromolecules* **2012**, *45*, 3740. (b) Khlyabich, P. P.; Burkhart, B.; Ng, C. F.; Thompson, B. C. *Macromolecules* **2011**, *44*, 5079.

(11) Burkhart, B.; Khlyabich, P. P.; Cakir Canak, T.; LaJoie, T. W.; Thompson, B. C. *Macromolecules* **2011**, *44*, 1242.

(12) Alstrup, J.; Jørgensen, M.; Medford, A. J.; Krebs, F. C. *ACS Appl. Mater. Interfaces* **2010**, *2*, 2819.

(13) Jeltsch, K. F.; Schädel, M.; Bonekamp, J.-B.; Niyamakom, P.; Rauscher, F.; Lademann, H. W. A.; Dumsch, I.; Allard, S.; Scherf, U.; Meerholz, K. *Adv. Funct. Mater.* **2012**, *22*, 397.

(14) Gurau, M. C.; Delongchamp, D. M.; Vogel, B. M.; Lin, E. K.; Fischer, D. A.; Sambasivan, S.; Richter, L. J. *Langmuir* **2007**, *23*, 834.

(15) Kotlarski, J. D.; Moet, D. J. D.; Blom, P. W. M. *J. Polym. Sci., Part B: Polym. Phys.* **2011**, *49*, 708.

(16) (a) Brabec, C. J.; Heeney, M.; McCulloch, I.; Nelson, J. *Chem. Soc. Rev.* **2011**, *40*, 1185. (b) van Bavel, S.; Veenstra, S.; Loos, J. *Macromol. Rapid Commun.* **2010**, *31*, 1835.

(17) Shrotriya, V.; Yao, Y.; Li, G.; Yang, Y. *Appl. Phys. Lett.* **2006**, *89*, 063505.

(18) Li, N.; Machui, F.; Waller, D.; Koppe, M.; Brabec, C. J. *Sol. Energy Mater. Sol. Cells* **2011**, *95*, 3465.